Electronic Supplementary Material (ESI) for RSC Advances

Optical stretching as a tool to investigate the mechanical properties of lipid bilayers

Solmaz et al.

Supplemental Information

GUV centering: GUVs were centered between the laser beams by manually adjusting the laser power. We examined all experimental records and measured the actual position of the GUV relative to the walls of the channel. We found that the GUV position varied from the precise channel center with a standard deviation of 3.58 μm. We computed the stress-strain profile for a typical GUV assuming perfect centering of the GUV and measured a κ of 6.30 ± 0.34 kT. If we assume the same GUV is off-center by 3.58 μm, we obtain a κ of 6.58 ± 0.42 kT.

Area strain calculation: We calculated the area strain of a GUV as follows. The grayscale image for each frame was processed using our in-house Matlab code to trace the edge of the GUV. The nominal edge is located at the grayscale center-of-mass in an 8-pixel region surrounding the darkest pixel at each point along the GUV circumference. The edge coordinates formed a closed contour for each frame. The nominal GUV center was located at the center of this contour.

The resulting contour data set for each image frame consists of the location of the contour center and a contour radius for each of 360 azimuthal angular points. Contour radius can be expressed as a function of azimuthal angle ($r = r(\theta)$).

We then proceeded to expand the contour data in Legendre polynomials. This strategy fits the shape of the contour as an expansion of the equatorial plane of a base sphere with radius R. This base sphere is the assumed "relaxed" shape of the untrapped GUV. To find R, the GUV at minimum trapping power is assumed to be a prolate sphereoid. The volume of this GUV is calculated as $V_0 = \frac{4}{3}\pi a^2 b$, where a is the semi-minor axis and b is the semi-major axis. R is then the radius of a sphere with the same volume as this prolate spheroid. Initial area is calculated as the surface area of this sphere, $A_0 = 4\pi R^2$. We restrict our Legendre expansion to the second mode coefficient (u_2), since this can be used to represent the shape change of the contour from circle to increasingly eccentric ellipse. We reconstructed the contour using the equation,

$$r(\theta) = R + u_2 P_2^0(\cos\theta) \,, \tag{1}$$

where

$$P_2^0(\cos\theta) = \frac{1}{2}(3\cos^2\theta - 1) \,, \tag{2}$$

and u_2, using the ortho-normality of the Legendre polynomials, is given by the integral:

$$u_2 = \frac{5}{2}\int P_2^0(\cos\theta)[r(\cos\theta) - R]d\theta. \tag{3}$$

After reconstruction the contour, the top half the contour (0-180°) was numerically integrated to generate a solid of rotation about its major axis corresponding to the surface area of the GUV.

$$A = 2\pi \int_0^{\pi} r \sin\theta \sqrt{r^2 + \left(\frac{dr}{d\theta}\right)^2}\, d\theta \qquad (4)$$

Area strain is calculated using, $\Delta A = \left(A - A_0\right)/A_0$.

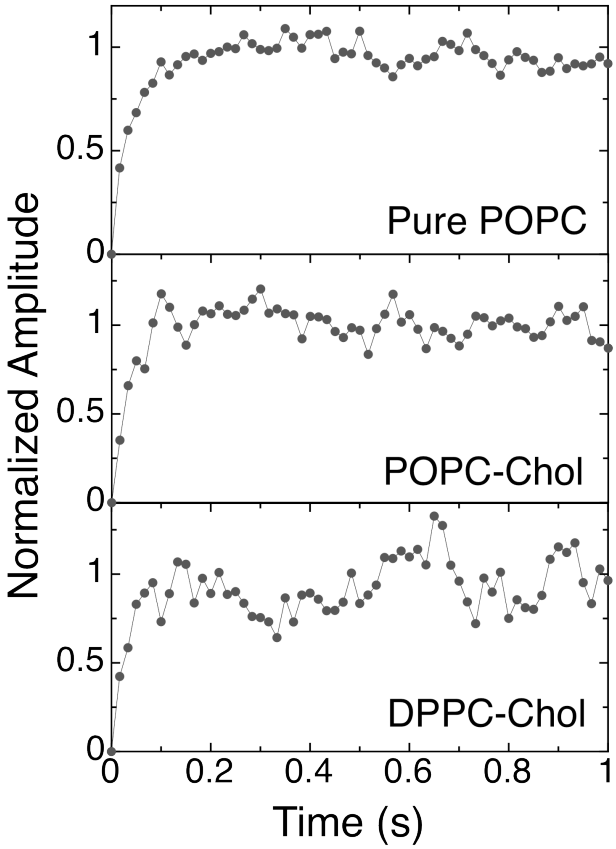

Figure S1. The averaged step response of GUVs for each population, showing the characteristic rise time.

Response time: The response time of a GUV to optical power increase was determined by considering each laser power increment in a stress strain experiment as a single step-response experiment. While there was too much noise to discern a time-dependent response by looking at each of these step-responses individually, noise could be reduced by averaging the normalized strain amplitude data for all step responses in a given population. A rise-time behavior was observed in these averaged data for each population, as shown in Figure S1. Each population achieved equilibrium strain after ~200 ms.

Calibration of optical power: The optical power of our DBOT setup was measured by tracking the velocity of polystyrene beads being pushed by single laser beams. We first trapped a polystyrene bead (n = 1.615) in water with equal power from both beams. We then displace the bead to one side of the channel by increasing the power of one beam. We then shut that beam off, allowing the particle to travel to the opposite side of the

channel, and record the distance vs. time. Where velocity was constant (i.e. terminal velocity was achieved), we found the laser force by setting it equal to the drag force $F_{drag} = 6\pi\eta\rho v$, where η is the viscosity of the water (0.0009 Pa·s at experimental temperature), ρ is the radius of polystyrene bead (4.97μm) and v is the velocity. To account for the geometry of the system, the following multiplicative correction factor was then applied to the drag force:

$$a = \frac{1}{1-\frac{9}{16}(\rho/b)+\frac{1}{8}(\rho/b)^3-\frac{45}{256}(\rho/b)^4-\frac{1}{16}(\rho/b)^5}\cdot\frac{2\eta+b\beta}{3\eta+b\beta},$$

where b is the distance to the closest wall and β^{-1} is the slip coefficient. The first term is associated with the proximity of the walls while the second term takes into account the slip-flow boundary conditions on the surface of the particle (reference 36 in the manuscript). The experiment was repeated with two different optical power levels, 50mW and 100mW. An upper limit on the measured force is given by corrected drag force assuming no-slip conditions ($\beta \to \infty$) while a lower limit is found in the case of perfect slip ($\beta \to 0$). In Figure S2 these boundaries were plotted against the theoretical optical forces. Our theoretical prediction of optical force falls within these boundaries, while the upper boundary matches the theoretical optical force within ~10% at the center of the channel.

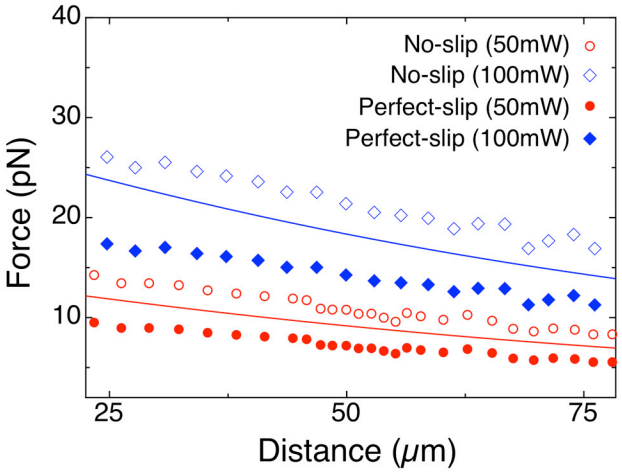

Figure S2. The drag forces in no-slip and perfect-slip cases are plotted against the calculated optical forces (solid lines) from one beam for two power levels, 50mW and 100mW. 50μm corresponds to the center of the channel.

We also repeated the full stress-strain calculation for select vesicles from our populations assuming an optical force 20% greater than that predicted by our ray optics model. We found that this change in total force magnitudes shifts the positions of the stress-strain curves, but does not significantly alter their slope, meaning that it does not change the calculated bending modulus (see Figure S3). This result is to be expected from analytical arguments. A constant scale factor in T_{equ} (Eq. 1 in the text) will scale $\boldsymbol{\sigma_h}$ by the same factor, corresponding to an overall shift of the stress-strain curve.

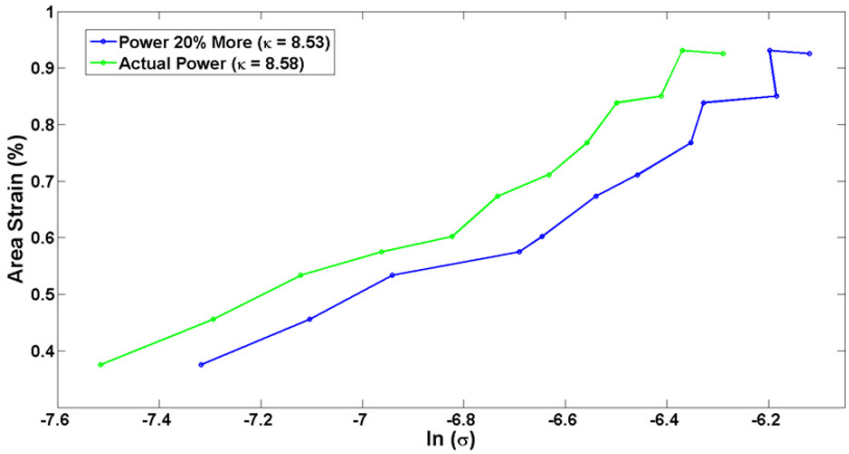

Figure S3. Example of the change to an observed stress-strain curve upon changing the force by ~20% (the approximate range shown in Figure S2). Note that while the curve shifts, its slope does not change significantly, meaning that the same value of bending modulus is returned regardless of the total magnitude of the force.

Measured σ_0 values: The σ_0 values are measured by finding the y-axis intercept of area-strain vs. applied lateral tension. We calculated these values for each GUV and present them as histograms for each population in Figure S4.

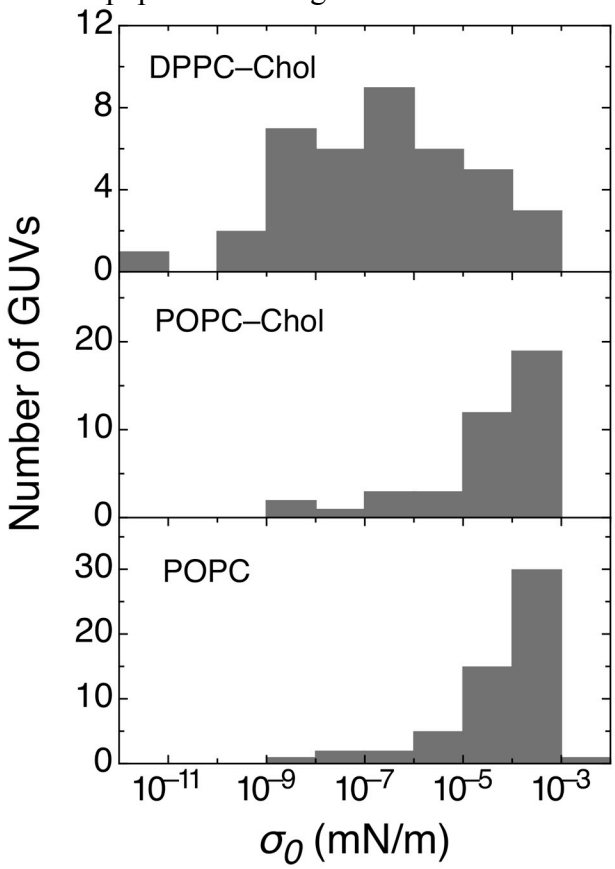

Figure S4. Histograms of measured initial tension (σ_0) values for each GUV population